Fully Kinetic Simulation of 3D Kinetic Alfvén Turbulence

Daniel Grošelj,[1] Alfred Mallet,[2] Nuno F. Loureiro,[3] and Frank Jenko[1]

[1]*Max-Planck-Institut für Plasmaphysik, Boltzmannstraße 2, D-85748 Garching, Germany*
[2]*Space Science Center, University of New Hampshire, Durham, NH 03824, USA*
[3]*Plasma Science and Fusion Center, Massachusetts Institute of Technology, Cambridge, MA 02139, USA*

(Dated: March 7, 2018)

We present results from a three-dimensional particle-in-cell simulation of plasma turbulence, resembling the plasma conditions found at kinetic scales of the solar wind. The spectral properties of the turbulence in the subion range are consistent with theoretical expectations for kinetic Alfvén waves. Furthermore, we calculate the local anisotropy, defined by the relation $k_\parallel(k_\perp)$, where $k_\parallel$ is a characteristic wave number along the local mean magnetic field at perpendicular scale $l_\perp \sim 1/k_\perp$. The subion range anisotropy is scale dependent with $k_\parallel < k_\perp$ and the ratio of linear to nonlinear time scales is of order unity, suggesting that the kinetic cascade is close to a state of critical balance. Our results compare favorably against a number of *in situ* solar wind observations and demonstrate—from first principles—the feasibility of plasma turbulence models based on a critically balanced cascade of kinetic Alfvén waves.

PACS numbers: 52.35.Ra, 94.05.Lk, 52.65.Rr, 96.50.Tf

Introduction.—Many space and astrophysical plasmas are found in a weakly collisional turbulent state, with prominent examples ranging from the solar wind [1], to more distant astrophysical environments such as accretion disks [2–4], galaxy clusters [5, 6], and the interstellar medium [7, 8]. In low-collisionality plasmas, the fluidlike inertial range energy cascade transitions into kinetic turbulence at the ion kinetic scales, with important implications for the turbulent heating of ions and electrons, and for the (bulk) transport properties of the plasma [2, 9–14]. The nature of the kinetic-scale plasma turbulence is, however, still a matter of debate [10, 11, 15–25]. The most detailed observational data originate from *in situ* solar wind measurements [20, 24–32], which thus provide the most stringent constraints for the theoretical predictions [10, 11, 33–36]. Spacecraft measurements have shown that the solar wind is highly turbulent, displaying power-law fluctuation spectra over a broad range of scales [1, 37, 38]. In the inertial range, above the proton kinetic scales, the magnetic energy follows an $E(k_\perp) \propto k_\perp^{-5/3}$ wave number spectrum in directions perpendicular to the local mean magnetic field, whereas the inferred spectrum parallel to the local mean field is steeper: $E(k_\parallel) \propto k_\parallel^{-2}$ [39–41]. Thus, solar wind turbulence is anisotropic. At kinetic scales, a break in the inertial range spectrum is observed, followed by a steeper power law with a spectral exponent around -2.8 at subproton scales [28, 29] for wave numbers nearly perpendicular to the mean field. Turbulence at kinetic scales remains anisotropic [29, 42], although presently available measurements limit the accuracy to which one can determine the kinetic-scale anisotropy.

An elegant explanation for the development of scale-dependent anisotropy can be given in terms of the critical balance conjecture [10, 11, 35, 38, 43–47]. This states that even when the turbulent plasma dynamics is strongly nonlinear, certain properties of linear wave physics are maintained, such that the nonlinear time at each scale is comparable to the characteristic time of the relevant linear mode. Therefore, linear theory may be used to aid theoretical predictions even in strongly turbulent regimes. In the inertial range of solar wind turbulence, most fluctuations display properties consistent with Alfvén waves (e.g., Refs. [27, 48]), thus motivating the use of magnetohydrodynamics (MHD) at scales larger than the proton gyroradius. On the other hand, the question regarding the most relevant linear modes in the kinetic range of the solar wind has been the subject of some controversy [10, 17–20, 24, 35, 49, 50]. The leading two wavelike models of kinetic-scale turbulence are presently the kinetic Alfvén wave (KAW) turbulence model [10, 11, 35] and the whistler wave turbulence model [33, 34, 51–54]. Upon balancing the linear wave crossing time with the nonlinear time, critical balance for both types of modes (KAWs and whistlers) predicts an anisotropy given by $k_\parallel \propto k_\perp^{1/3}$, assuming that possible corrections due to intermittency and dissipative effects can be neglected [10, 11, 52]. Here, $k_\parallel$ should be understood as a characteristic wave number along the *local* mean magnetic field [44] at perpendicular scale $l_\perp \sim 1/k_\perp$. Observational evidence suggests that the kinetic-scale fluctuations are predominantly of KAW type [20, 27, 29, 31], although there also exists some evidence in support of whistler waves [24, 55].

Complementary to observations and theory, numerical simulations of kinetic-scale solar wind turbulence have attracted a great deal of interest [15, 21, 22, 49, 53, 56–70]. However, capturing the entire range of kinetic physics in a turbulent simulation has proven difficult due to the immense computational requirements of the problem. For this reason, a number of previous works employed various simplifications of the first-principles kinetic description in three spatial dimensions. These simplifications typically involve various reduced-kinetic approximations [15, 21, 60, 64, 69] and/or restrictions to a two-dimensional geometry [21, 49, 53, 58, 63, 70]. Only recently have fully kinetic, three-dimensional (3D) simulations become computationally accessible [22, 61, 67, 71, 72]. Previous works employing 3D fully

kinetic simulations were aimed at different aspects such as whistler wave turbulence [61, 67], intermittent heating [22], particle acceleration in the highly relativistic regime [71], or bulk plasma heating by KAW turbulence [72]. Thus, even though there exists observational evidence for the transition into KAW turbulence at kinetic scales [20, 27, 29, 31], supplemented by evidence of critical balance in gyrokinetic [46], electron MHD [52, 56], and Landau fluid simulations [73], the natural occurrence of the transition has to our knowledge never been convincingly demonstrated in a 3D fully kinetic simulation.

In this Letter, we try to fill in a long-standing gap in the literature, and perform a 3D fully kinetic plasma turbulence simulation in order to demonstrate the feasibility of the critically balanced KAW turbulence model from first principles. Using a simulation setup broadly resembling the typical conditions at the tail of the MHD inertial range and at subion scales of the slow solar wind, we show that the ratios of the turbulent spectra between ion and electron scales are consistent with theoretical expectations for KAWs. Furthermore, we perform a first-time direct calculation of the *local* scale-dependent anisotropy in a 3D kinetic simulation of sub-ion-scale plasma turbulence. From the anisotropy, we infer the ratio of linear to nonlinear time scales and obtain an order unity estimate in the subion range, suggesting that the kinetic cascade is close to a state of critical balance.

Simulation details.—The triply periodic simulation box dimensions in units of the ion inertial length d_i are $L_\perp = 16.97d_i$ and $L_z = 42.43d_i$ in directions perpendicular and parallel to the mean magnetic field $\mathbf{B}_0 = B_0\hat{\mathbf{e}}_z$, respectively. The initial condition is similar to the one used in Ref. [74] and consists of counterpropagating Alfvén waves with wave numbers $(k_{\perp,0}, 0, \pm k_{z,0})$, $(0, k_{\perp,0}, \pm k_{z,0})$, and $(2k_{\perp,0}, 0, \pm k_{z,0})$, where $k_{\perp,0} = 2\pi/L_\perp$ and $k_{z,0} = 2\pi/L_z$. A different phase is used for each mode. "Alfvén waves" are to be understood here in the usual sense of MHD with corresponding perpendicular fluid velocity $\delta\mathbf{u}_\perp$ and magnetic field $\delta\mathbf{B}_\perp$ perturbations. Each pair of counterpropagating waves has equal amplitudes, such that the mean cross-helicity $H_c = \langle\delta\mathbf{u}\cdot\delta\mathbf{B}\rangle$ is zero (results from a second simulation with nonvanishing cross-helicity are included in Supplemental Material [75]). Ions and electrons have an initial Maxwellian velocity distribution with equal temperatures T_0 and uniform densities n_0, corresponding to a thermal velocity $v_{\mathrm{th},i} = \sqrt{2T_0/m_i} = 0.031c$ for ions and $v_{\mathrm{th},e} = \sqrt{2T_0/m_e} = 0.25c$ for electrons [76], where c is the light speed, m_i is the ion mass, and m_e is the electron mass. We also initialize a self-consistent electric current according to $\mathbf{J} = (c/4\pi)\nabla\times\delta\mathbf{B}_\perp$. A reduced ion-electron mass ratio of $m_i/m_e = 64$ is used and the electron plasma to cyclotron frequency ratio is $\omega_{pe}/\Omega_{ce} = 2.83$. The ion plasma beta is $\beta_i = 8\pi n_0 T_0/B_0^2 = 0.5$. The initial turbulence amplitude $\epsilon = \delta B/B_0 = \delta u/v_A$, where $v_A = B_0/\sqrt{4\pi n_0 m_i}$ is the Alfvén speed, δu is the root-mean-square fluid velocity, and δB is the root-mean-square fluctuating magnetic field, is chosen such as to satisfy the critical balance condition ($k_\perp\delta B = k_\parallel B_0$) at the box scale: $\epsilon = L_\perp/L_z = 0.4$.

The physical setup resembles the plasma conditions inferred from solar wind measurements [27, 38, 41, 42] in the following ways: (i) an anisotropy is imposed at the box scale ($k_{z,0} < k_{\perp,0}$), (ii) the initial condition consists of counterpropagating, oblique Alfvén waves, (iii) the initial turbulence amplitude is chosen such as to satisfy critical balance, and (iv) the plasma parameters are similar to those typically found in the solar wind (plasma beta and ion-electron temperature ratio both of order unity).

We perform the simulation using the particle-in-cell code OSIRIS [77, 78]. The spatial resolution is $(N_x, N_y, N_z) = (768, 768, 1536)$. We employ on average 64 particles per cell per species. The charge distribution of each finite-size particle is represented by third-order cubic splines [79], which improve energy conservation and reduce the relative amount of particle noise compared to lower-order splines [80, 81]. At each step, we also apply a second-order compensated binomial filter [79] on the electric current and on the electromagnetic fields felt by the particles. The total energy increase due to numerical heating is kept below 0.033% during the entire simulation. To reduce particle noise, the data used for the spectral and scale-dependent anisotropy analysis is short-time averaged over a time window of duration $\Delta t = 2.4\Omega_{ce}^{-1}$, where $\Omega_{ce} = e_0 B_0/(m_e c)$ and e_0 is the elementary charge.

Global evolution.—The global evolution during the turbulent decay is illustrated in Fig. 1 by plotting the mean fluctuating magnetic energy and the mean-square electric current versus time. We take the box-scale Alfvén transit time, $t_A = L_z/v_A$, as the basic time unit. The markers in Fig. 1(b) are used to indicate the times at which we analyze the turbulence spectral properties in what follows. The magnetic energy decreases throughout the simulation as a result of ion and electron heating. By the end of the simulation, the species internal energy increases by 17% for ions and by 15% for electrons (relative to the value at $t = 0$), whereas the bulk fluid energy decreases by 76%. On the other hand, the electric current undergoes an initial transient, during which it is rapidly amplified, before it eventually starts to decrease. The rapid current amplification can be attributed to current sheet formation [13, 21]. Indeed, a visual inspection of the 3D structure of the electric current (not shown here) reveals that the turbulent structures are mainly sheetlike (see Supplemental Material [75] for an animation, showing how the current sheets form).

Turbulent spectra and spectral ratios.—We compute the one-dimensional perpendicular wave number spectra $E(k_\perp)$ by summing the squared amplitudes of Fourier modes contained in a given perpendicular wave number shell of width $\Delta k_\perp = 2\pi/L_\perp$, followed by an average along the z direction. The shells are nonoverlapping and centered at integer values of $\Delta k_\perp$. We approximate the perpendicular wave vectors as $\mathbf{k}_\perp \approx (k_x, k_y)$. That is, the perpendicular direction is defined with respect to $\mathbf{B}_0$ [82]. In Fig. 2 we show the spectra of the magnetic ($\delta\mathbf{B}$), perpendicular electric ($\mathbf{E}_\perp$), and electron density fluctuations (δn_e) at time $t_1 = 0.71t_A$. Similar results are obtained at later stages of the turbulent decay (not shown here)
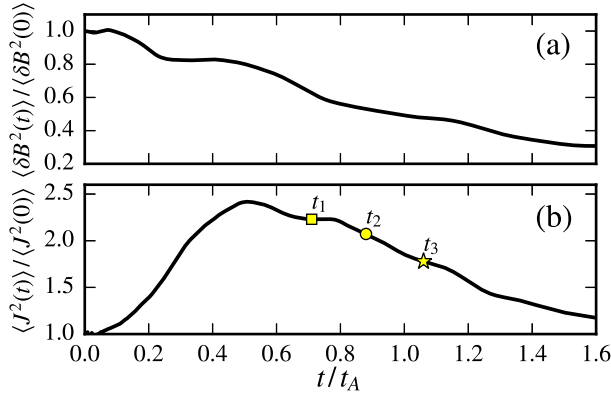
Figure 1. Time evolution of the mean magnetic energy (a) and of the mean-square electric current (b). The curves are normalized to the values at $t = 0$. The markers in panel (b) denote the times at which we analyze the spectral properties ($t_1/t_A = 0.71, t_2/t_A = 0.88, t_3/t_A = 1.06$).

Figure 2. One-dimensional $k_\perp$ spectra of magnetic, perpendicular electric, and density fluctuations at time $t_1 = 0.71 t_A$. The -2.8 slope is shown for reference. Gray shading is used to indicate the range of scales dominated by particle noise.

at times t_2 and t_3 marked in Fig. 1. Dotted vertical lines are used in Fig. 2 to indicate various kinetic scales: the species inertial length $d_s = c/\omega_{ps}$, where $\omega_{ps} = \sqrt{4\pi e_0^2 n_0/m_s}$ and $s = i, e$ is the species index, the species Larmor radius $\rho_s = v_{\text{th},s}/\Omega_{cs}$, where $\Omega_{cs} = e_0 B_0/(m_s c)$, and the Debye scale $\lambda_D = v_{\text{th},e}/(\omega_{pe}\sqrt{2})$. The sub-ion-scale spectra are in relatively good agreement with a number of observational studies [20, 27–29], albeit with some limitations due to the reduced ion-electron mass ratio in our simulation. In particular, the local slope of the magnetic energy spectrum is consistent with the typical values of spectral exponents observed in the solar wind [28, 29], even though a well-defined sub-ion-scale power law cannot be established. The lack of a well-defined power law, should one in fact exist, can presumably be attributed to the proximity of electron kinetic scales, which may cause a steepening of the spectral slope due to collisionless damping via the electron Landau resonance [10, 60, 64, 68, 70]. Indeed, solar wind observations [28] and gyrokinetic simulations [60, 64] with realistic proton-electron mass ratios show a steepening of the magnetic energy spectra as the wave number approaches the electron scales.

Looking at the results for δn_e and $\mathbf{E}_\perp$, we find that the electric field spectrum flattens in the kinetic range and separates from the magnetic energy, whereas the density spectrum converges toward a near equipartition with the magnetic spectrum in appropriately normalized units [20, 35]. Both of these features are in agreement with solar wind observations [20, 27]. Most importantly, the near equipartition among density and magnetic fluctuations in the subion range is a key property of KAWs, as opposed to the weakly compressible $((|\delta n_e|/n_0)^2 \ll (|\delta B|/B_0)^2)$ whistler waves [20, 35, 54]. In the asymptotic limit

$$1/\rho_i \ll k_\perp \ll 1/\rho_e, \qquad k_\parallel \ll k_\perp, \qquad (1)$$

assuming singly charged ions, and equal ion and electron temperatures, the analytical prediction for KAWs reads [35]
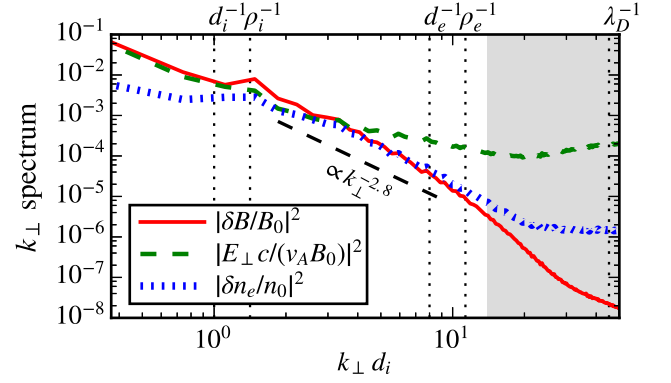
$(\beta_i + 2\beta_i^2)(|\delta n_e|/n_0)^2 \sim (|\delta B|/B_0)^2$. Thus, for $\beta_i = 0.5$ we have $(|\delta n_e|/n_0)^2 \sim (|\delta B|/B_0)^2$, in agreement with our results presented in Fig. 2. The difference between the density and magnetic energy spectral slopes seen in Fig. 2 is a trend not captured by the asymptotic prediction. It is, however, fully consistent with results from nonlinear gyrokinetic simulations [70].

To further demonstrate that the sub-ion-scale fluctuations are consistent with theoretical expectations for KAWs, we consider the following ratios of the one-dimensional spectra [11, 35, 54, 70]:

$$\frac{(|E_\perp|c/v_A)^2}{|\delta B_\perp|^2} \sim \frac{(k_\perp \rho_i)^2}{4 + 4\beta_i}, \qquad \frac{(|\delta n_e|/n_0)^2}{(|\delta B_\parallel|/B_0)^2} \sim \frac{1}{\beta_i^2},$$

$$\frac{|\delta B_\parallel|^2}{|\delta B|^2} \sim \frac{\beta_i}{1 + 2\beta_i}. \qquad (2)$$

The above expressions are obtained from linearized kinetic equations in the limit (1) for singly charged ions, and equal ion and electron temperatures. The turbulence spectral ratios are compared against the analytical predictions in Fig. 3 [83]. Good agreement between the linear KAW theory and the simulation is found for all ratios. The results are also in good agreement with nonlinear gyrokinetic simulations [70]. Considering the fact that the initial fluctuation amplitude in our simulation is relatively large, our simulation box is only moderately elongated along z, and the ion-electron mass ratio has been reduced, the agreement with theoretical predictions is quite remarkable and indicates a certain robustness of the KAW cascade, beyond the limits of gyrokinetic theory, in the context of which KAW turbulence has most frequently been studied [14, 15, 60, 64].

Scale-dependent anisotropy.—Finally, we consider the local scale-dependent anisotropy of the kinetic turbulence. We employ the method introduced by Cho and Lazarian [52, 56], which we summarize here briefly as follows. At a given perpendicular wave number $k_\perp$, we define a local mean magnetic field $\mathbf{B}_{0,k_\perp}$ and a local fluctuating field $\delta\mathbf{B}_{k_\perp}$. The local
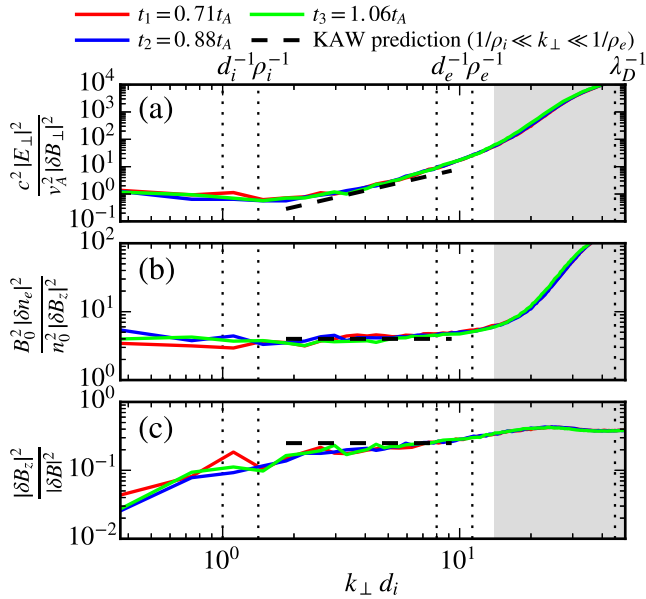
Figure 3. Ratios of the $k_\perp$ spectra obtained from the simulation (solid lines; see text for further details). Dashed lines show the analytical predictions for KAWs [11, 35].

mean field is obtained by eliminating the Fourier modes with perpendicular wave numbers greater than $k_\perp/2$ and the fluctuating field is obtained by eliminating the modes with wave numbers less than $k_\perp/2$ or greater than $2k_\perp$. The characteristic local parallel wave number $k_\parallel$ at scale $l_\perp \sim 1/k_\perp$ is then approximated as [56]

$$k_\parallel \approx \left(\frac{\langle |\mathbf{B}_{0,k_\perp} \cdot \nabla \delta \mathbf{B}_{k_\perp}|^2 \rangle}{\langle B_{0,k_\perp}^2 \rangle \langle \delta B_{k_\perp}^2 \rangle} \right)^{1/2}, \qquad (3)$$

where $\langle \ldots \rangle$ represents a space average. In addition, we estimate the nonlinearity parameter $\chi \approx k_\perp \langle \delta B_{\perp,k_\perp}^2 \rangle^{1/2} / (k_\parallel B_0)$ [10, 11, 52], which can be regarded as an approximation for the ratio of linear (KAW) and nonlinear time scales. For a critically balanced cascade, it is expected by definition that $\chi \sim 1$. The results are shown in Fig. 4. Over a limited subion range, the anisotropy scaling is broadly consistent with the standard critical balance prediction, $k_\parallel \propto k_\perp^{1/3}$ [10, 11], although the scale separation in the simulation is to small to determine the scaling precisely. The estimated nonlinearity parameter is order unity at subion scales and exhibits a weak dependence on $k_\perp$. The scale dependence of χ could be possibly attributed to dissipative effects and/or intermittency [57]. Moreover, supposing linear modes other than KAWs are energetically significant, they could bias the anisotropy estimation of the KAW portion of the cascade. Within the limits of the spectral ratios analysis, we do not find evidence for the latter possibility. We also confirmed that the anisotropy does not change significantly upon inclusion of a moderate mean cross-helicity (see Supplemental Material [75]). The question whether or not our conclusions are influenced by the reduced ion-electron mass

ratio of 64 or by the lack of an external turbulence forcing is left for future studies. Nonetheless, the local scale-dependent anisotropy calculation performed in this work provides the first reference values obtained from a 3D fully kinetic simulation of KAW turbulence.
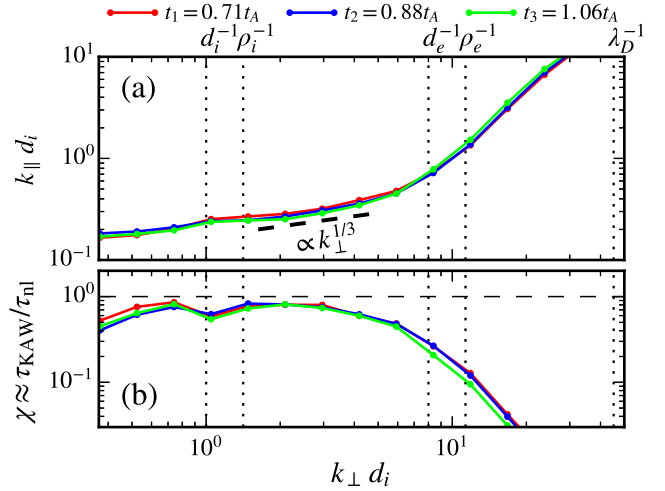

Figure 4. Scale-dependent anisotropy with respect to the direction of the *local* mean magnetic field (a) and the scale-dependent ratio of the linear (KAW) and nonlinear time scales (b). The 1/3 slope in panel (a) is shown for reference.

Discussion and conclusions.—This Letter presents a 3D fully kinetic simulation of plasma turbulence under conditions relevant to the solar wind. We show that the spectral properties in the subion range are consistent with theoretical expectations for KAWs. The initial perturbations at the start of the simulation are restricted to scales above the ion inertial length. Furthermore, the initially excited Alfvén waves are only moderately oblique. Therefore, it is not obvious from a theoretical perspective that kinetic Alfvén fluctuations should dominate at subion scales. Other possibilities, such as whistler wave turbulence, cannot be ruled out. However, that is not what we observe. A direct calculation of the local scale-dependent anisotropy is also performed. This allows for an estimate of the nonlinearity parameter χ, which is in broad agreement with critical balance ($\chi \sim 1$) at subion scales [10, 11].

Our work has important implications for the fundamental understanding of kinetic turbulence in weakly collisional plasmas, such as the solar wind, where a number of experimental studies already support the KAW turbulence scenario [20, 27, 29, 31]. Several alternatives or extensions of the KAW turbulence theory have been considered, such as a transition to whistler turbulence deep in the subion range [17, 18], or reconnection-mediated kinetic turbulence [84–87]. Given that our simulation covers only a moderate range of scales, it is presently difficult to assess the hypothetical role of these features and a definitive answer is left for future works. In this Letter we demonstrated that, even when the full range of 3D kinetic physics is retained, the phenomenology of critically balanced KAW turbulence remains highly relevant. Thus, the

KAW turbulence theory seems to provide at least a reasonable starting point, upon which more refined models could be built.

[1] R. Bruno and V. Carbone, Living Rev. Solar Phys. **10**, 2 (2013).
[2] E. Quataert and A. Gruzinov, Astrophys. J. **520**, 248 (1999).
[3] P. Sharma, E. Quataert, G. W. Hammett, and J. M. Stone, Astrophys. J. **667**, 714 (2007).
[4] M. W. Kunz, J. M. Stone, and E. Quataert, Phys. Rev. Lett. **117**, 235101 (2016).
[5] T. J. Dennis and B. D. G. Chandran, Astrophys. J. **622**, 205 (2005).
[6] I. Zhuravleva, E. Churazov, A. A. Schekochihin, S. W. Allen, P. Arévalo, A. C. Fabian, W. R. Forman, J. S. Sanders, A. Simionescu, R. Sunyaev, A. Vikhlinin, and N. Werner, Nature (London) **515**, 85 (2014).
[7] J. W. Armstrong, B. J. Rickett, and S. R. Spangler, Astrophys. J. **443**, 209 (1995).
[8] Y. Lithwick and P. Goldreich, Astrophys. J. **562**, 279 (2001).
[9] S. R. Cranmer and A. A. van Ballegooijen, Astrophys. J. **594**, 573 (2003).
[10] G. G. Howes, S. C. Cowley, W. Dorland, G. W. Hammett, E. Quataert, and A. A. Schekochihin, J. Geophys. Res. **113**, A05103 (2008).
[11] A. A. Schekochihin, S. C. Cowley, W. Dorland, G. W. Hammett, G. G. Howes, E. Quataert, and T. Tatsuno, Astrophys. J. Suppl. Ser. **182**, 310 (2009).
[12] B. D. G. Chandran, T. J. Dennis, E. Quataert, and S. D. Bale, Astrophys. J. **743**, 197 (2011).
[13] W. H. Matthaeus, M. Wan, S. Servidio, A. Greco, K. T. Osman, S. Oughton, and P. Dmitruk, Phil. Trans. R. Soc. A **373**, 20140154 (2015).
[14] A. Bañón Navarro, B. Teaca, D. Told, D. Groselj, P. Crandall, and F. Jenko, Phys. Rev. Lett. **117**, 245101 (2016).
[15] G. G. Howes, W. Dorland, S. C. Cowley, G. W. Hammett, E. Quataert, A. A. Schekochihin, and T. Tatsuno, Phys. Rev. Lett. **100**, 065004 (2008).
[16] W. H. Matthaeus, S. Servidio, and P. Dmitruk, Phys. Rev. Lett. **101**, 149501 (2008).
[17] D. Shaikh and G. P. Zank, Mon. Not. R. Astron. Soc. **400**, 1881 (2009).
[18] J. J. Podesta, J. E. Borovsky, and S. P. Gary, Astrophys. J. **712**, 685 (2010).
[19] J. J. Podesta, J. Geophys. Res. **117**, A07101 (2012).
[20] C. H. K. Chen, S. Boldyrev, Q. Xia, and J. C. Perez, Phys. Rev. Lett. **110**, 225002 (2013).
[21] S. Servidio, F. Valentini, D. Perrone, A. Greco, F. Califano, W. H. Matthaeus, and P. Veltri, J. Plasma Phys. **81**, 325810107 (2015).
[22] M. Wan, W. H. Matthaeus, V. Roytershteyn, H. Karimabadi, T. Parashar, P. Wu, and M. Shay, Phys. Rev. Lett. **114**, 175002 (2015).
[23] G. G. Howes, Phil. Trans. R. Soc. A **373**, 20140145 (2015).
[24] Y. Narita, R. Nakamura, W. Baumjohann, K.-H. Glassmeier, U. Motschmann, B. Giles, W. Magnes, D. Fischer, R. B. Torbert, C. T. Russell, R. J. Strangeway, J. L. Burch, Y. Nariyuki, S. Saito, and S. P. Gary, Astrophys. J. Lett. **827**, L8 (2016).
[25] D. Perrone, O. Alexandrova, A. Mangeney, M. Maksimovic, C. Lacombe, V. Rakoto, J. C. Kasper, and D. Jovanovic, Astrophys. J. **826**, 196 (2016).
[26] R. J. Leamon, C. W. Smith, N. F. Ness, W. H. Matthaeus, and H. K. Wong, J. Geophys. Res. **103**, 4775 (1998).
[27] S. D. Bale, P. J. Kellogg, F. S. Mozer, T. S. Horbury, and H. Reme, Phys. Rev. Lett. **94**, 215002 (2005).
[28] O. Alexandrova, J. Saur, C. Lacombe, A. Mangeney, J. Mitchell, S. J. Schwartz, and P. Robert, Phys. Rev. Lett. **103**, 165003 (2009).
[29] F. Sahraoui, M. L. Goldstein, G. Belmont, P. Canu, and L. Rezeau, Phys. Rev. Lett. **105**, 131101 (2010).
[30] K. T. Osman, W. H. Matthaeus, A. Greco, and S. Servidio, Astrophys. J. Lett. **727**, L11 (2011).
[31] C. S. Salem, G. G. Howes, D. Sundkvist, S. D. Bale, C. C. Chaston, C. H. K. Chen, and F. S. Mozer, Astrophys. J. Lett. **745**, L9 (2012).
[32] A. Chasapis, A. Retinò, F. Sahraoui, A. Vaivads, Y. V. Khotyaintsev, D. Sundkvist, A. Greco, L. Sorriso-Valvo, and P. Canu, Astrophys. J. Lett. **804**, L1 (2015).
[33] S. Galtier and A. Bhattacharjee, Phys. Plasmas **10**, 3065 (2003).
[34] S. Galtier, J. Plasma Phys. **72**, 721 (2006).
[35] S. Boldyrev, K. Horaites, Q. Xia, and J. C. Perez, Astrophys. J. **777**, 41 (2013).
[36] T. Passot and P. L. Sulem, Astrophys. J. Lett. **812**, L37 (2015).
[37] K. H. Kiyani, K. T. Osman, and S. Chapman, Phil. Trans. R. Soc. A **373**, 20140155 (2015).
[38] C. H. K. Chen, J. Plasma Phys. **82**, 535820602 (2016).
[39] T. S. Horbury, M. Forman, and S. Oughton, Phys. Rev. Lett. **101**, 175005 (2008).
[40] J. J. Podesta, Astrophys. J. **698**, 986 (2009).
[41] R. T. Wicks, T. S. Horbury, C. H. K. Chen, and A. A. Schekochihin, Mon. Not. R. Astron. Soc. **407**, L31 (2010).
[42] C. H. K. Chen, T. S. Horbury, A. A. Schekochihin, R. T. Wicks, O. Alexandrova, and J. Mitchell, Phys. Rev. Lett. **104**, 255002 (2010).
[43] P. Goldreich and S. Sridhar, Astrophys. J. **438**, 763 (1995).
[44] J. Cho and E. Vishniac, Astrophys. J. **539**, 273 (2000).
[45] J. Maron and P. Goldreich, Astrophys. J. **554**, 1175 (2001).
[46] J. M. TenBarge and G. G. Howes, Phys. Plasmas **19**, 055901 (2012).
[47] A. Mallet, A. A. Schekochihin, and B. D. G. Chandran, Mon. Not. R. Astron. Soc. **449**, L77 (2015).
[48] J. W. Belcher and L. Davis, J. Geophys. Res. **76**, 3534 (1971).
[49] D. Verscharen, E. Marsch, U. Motschmann, and J. Müller, Phys. Plasmas **19**, 022305 (2012).
[50] F. Sahraoui, G. Belmont, and M. L. Goldstein, Astrophys. J. **748**, 100 (2012).
[51] O. Stawicki, S. P. Gary, and H. Li, J. Geophys. Res. **106**, 8273 (2001).
[52] J. Cho and A. Lazarian, Astrophys. J. Lett. **615**, L41 (2004).

[53] S. Saito, S. P. Gary, H. Li, and Y. Narita, Phys. Plasmas **15**, 102305 (2008).

[54] S. P. Gary and C. W. Smith, J. Geophys. Res. **114**, A12105 (2009).

[55] C. Perschke, Y. Narita, S. P. Gary, U. Motschmann, and K.-H. Glassmeier, Ann. Geophys. **31**, 1949 (2013).

[56] J. Cho and A. Lazarian, Astrophys. J. **701**, 236 (2009).

[57] S. Boldyrev and J. C. Perez, Astrophys. J. Lett. **758**, L44 (2012).

[58] P. Wu, S. Perri, K. Osman, M. Wan, W. H. Matthaeus, M. A. Shay, M. L. Goldstein, H. Karimabadi, and S. Chapman, Astrophys. J. Lett. **763**, L30 (2013).

[59] H. Karimabadi, V. Roytershteyn, M. Wan, W. H. Matthaeus, W. Daughton, P. Wu, M. Shay, B. Loring, J. Borovsky, E. Leonardis, S. C. Chapman, and T. K. M. Nakamura, Phys. Plasmas **20**, 012303 (2013).

[60] J. M. TenBarge, G. G. Howes, and W. Dorland, Astrophys. J. **774**, 139 (2013).

[61] O. Chang, S. P. Gary, and J. Wang, Phys. Plasmas **21**, 052305 (2014).

[62] B. J. Vasquez, S. A. Markovskii, and B. D. G. Chandran, Astrophys. J. **788**, 178 (2014).

[63] F. Valentini, S. Servidio, D. Perrone, F. Califano, W. H. Matthaeus, and P. Veltri, Phys. Plasmas **21**, 082307 (2014).

[64] D. Told, F. Jenko, J. M. TenBarge, G. G. Howes, and G. W. Hammett, Phys. Rev. Lett. **115**, 025003 (2015).

[65] L. Franci, S. Landi, L. Matteini, A. Verdini, and P. Hellinger, Astrophys. J. **812**, 21 (2015).

[66] T. Parashar and W. H. Matthaeus, Astrophys. J. **832**, 57 (2016).

[67] S. P. Gary, R. S. Hughes, and J. Wang, Astrophys. J. **816**, 102 (2016).

[68] S. Kobayashi, F. Sahraoui, T. Passot, D. Laveder, P. L. Sulem, S. Y. Huang, P. Henri, and R. Smets, Astrophys. J. **839**, 122 (2017).

[69] S. S. Cerri, S. Servidio, and F. Califano, Astrophys. J. Lett. **846**, L18 (2017).

[70] D. Grošelj, S. S. Cerri, A. Bañón Navarro, C. Willmott, D. Told, N. F. Loureiro, F. Califano, and F. Jenko, Astrophys. J. **847**, 28 (2017).

[71] V. Zhdankin, G. R. Werner, D. A. Uzdensky, and M. C. Begelman, Phys. Rev. Lett. **118**, 055103 (2017).

[72] R. S. Hughes, S. P. Gary, J. Wang, and T. N. Parashar, Astrophys. J. Lett. **847**, L14 (2017).

[73] P. L. Sulem, T. Passot, D. Laveder, and D. Borgogno, Astrophys. J. **818**, 66 (2016).

[74] T. C. Li, G. G. Howes, K. G. Klein, and J. M. TenBarge, Astrophys. J. Lett. **832**, L24 (2016).

[75] See Supplemental Material at http://link.aps.org/supplemental/10.1103/PhysRevLett.120.105101, which includes Refs. [88, 89], for an animation of the turbulent dynamics and for results from a second simulation with nonvanishing mean cross-helicity.

[76] A recent study [70], using $v_{\mathrm{th},i} = 0.019c$ and $v_{\mathrm{th},e} = 0.19c$, found excellent agreement between two-dimensional (relativistic) fully kinetic and (nonrelativistic) gyrokinetic turbulence simulations at sub-ion scales for $\beta_i = 0.5$. Similarly, a study of the whistler anisotropy instability [90], using $0.035c \leq v_{\mathrm{th},e} \leq 0.14c$, found no clear physical dependence on $v_{\mathrm{th},e}$ for a fixed β_e. Thus, we do not expect significant modifications of our results due to artificially large thermal velocities.

[77] R. A. Fonseca, L. O. Silva, F. S. Tsung, V. K. Decyk, W. Lu, C. Ren, W. B. Mori, S. Deng, S. Lee, T. Katsouleas, and J. C. Adam, Lecture Notes in Comput. Sci. **2331**, 342 (2002).

[78] R. A. Fonseca, S. F. Martins, L. O. Silva, J. W. Tonge, F. S. Tsung, and W. B. Mori, Plasma Phys. Control. Fusion **50**, 124034 (2008).

[79] C. K. Birdsall and A. B. Langdon, *Plasma Physics via Computer Simulation* (Taylor & Francis Group, New York, 2005).

[80] E. Cormier-Michel, B. A. Shadwick, C. G. R. Geddes, E. Esarey, C. B. Schroeder, and W. P. Leemans, Phys. Rev. E **78**, 016404 (2008).

[81] P. A. Muñoz, P. Kilian, and J. Büchner, Phys. Plasmas **21**, 112106 (2014).

[82] The definition is consistent with previous works [44–46] and is motivated by the fact that the local $\mathbf{k}_\perp$ is to lowest order in $\epsilon = \delta B/B_0$ equal to (k_x, k_y), whereas, even to lowest order in ϵ, k_z cannot be considered representative for the local $k_\parallel$ [45, 46].

[83] Since the predictions involving the parallel field $\delta B_\parallel$ are independent of $\mathbf{k}$ and are not expected to give more than just the correct order of magnitude, we approximate the spectral ratios using δB_z instead of $\delta B_\parallel$.

[84] S. S. Cerri and F. Califano, New J. Phys. **19**, 025007 (2017).

[85] A. Mallet, A. A. Schekochihin, and B. D. G. Chandran, J. Plasma Phys. **83**, 905830609 (2017).

[86] N. F. Loureiro and S. Boldyrev, Astrophys. J. **850**, 182 (2017).

[87] L. Franci, S. S. Cerri, F. Califano, S. Landi, E. Papini, A. Verdini, L. Matteini, F. Jenko, and P. Hellinger, Astrophys. J. Lett. **850**, L16 (2017).

[88] Y. Lithwick, P. Goldreich, and S. Sridhar, Astrophys. J. **655**, 269 (2007).

[89] A. Beresnyak and A. Lazarian, Astrophys. J. **682**, 1070 (2008).

[90] R. S. Hughes, J. Wang, V. K. Decyk, and S. P. Gary, Phys. Plasmas **23**, 042106 (2016).